

Figure 6 Additional results of the simulation of the sEMG-controlled elbow orthosis. **A)** Raw sEMG signals used as input for the simulation. Specifically the three MVICs of the biceps (blue; $MVIC_{b1}$, $MVIC_{b2}$, $MVIC_{b3}$) and the three MVICs of the triceps (red; $MVIC_{t1}$, $MVIC_{t2}$, $MVIC_{t3}$). **B)** Envelopes of the raw sEMG signals of the biceps (blue) and triceps (red). **C)** Estimated muscle torque of the biceps (blue) and triceps (red) obtained by multiplying the envelopes multiplying by the mapping gains K_b and K_t . **D)** Estimated elbow torque calculated by subtracting the estimated triceps torque from the estimated biceps torque (Eq 4). **E)** Angular velocity resulting from the admittance model (Eq 5). **F)** Elbow angle displacement resulting from the integral of the angular velocity (Eq 5).

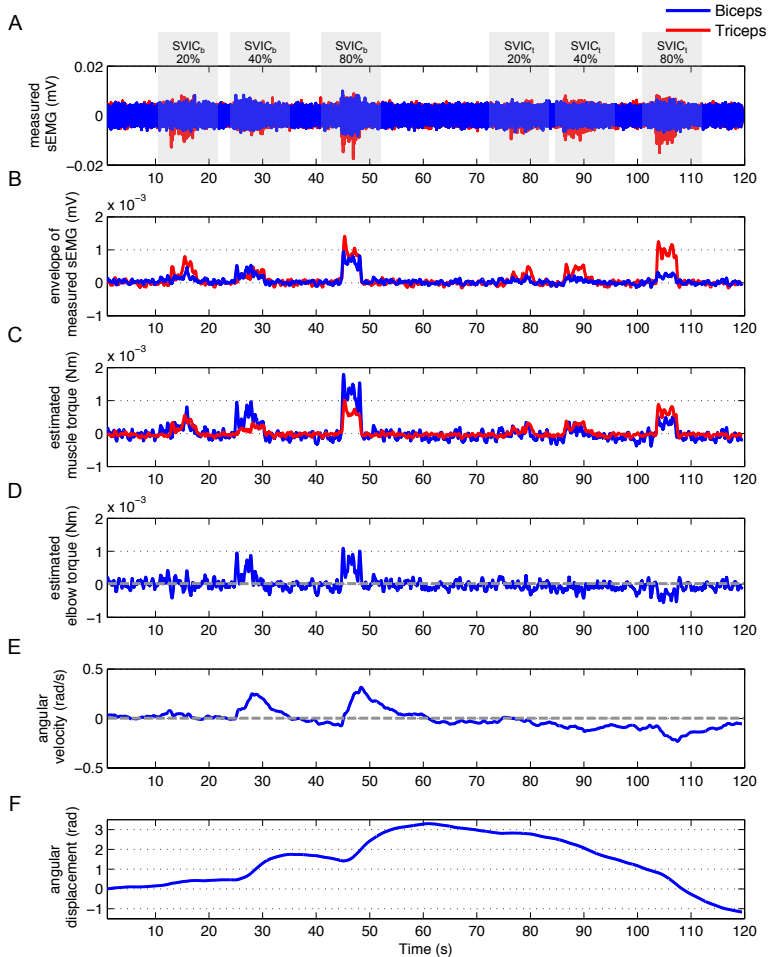


Figure 7 Additional results of the simulation of the sEMG-controlled elbow orthosis. **A)** Raw sEMG signals used as input for the simulation. Specifically the three SVIC of the biceps (blue; $SVIC_b$ 20%, $SVIC_b$ 40%, $SVIC_b$ 80%) and the three SVICs of the triceps (red; $SVIC_t$ 20%, $SVIC_t$ 40%, $SVIC_t$ 80%). **B)** Envelopes of the raw sEMG signals of the biceps (blue) and triceps (red) obtained by multiplying the envelopes multiplying by the mapping gains K_b and K_t . **D)** Estimated elbow torque calculated by subtracting the estimated triceps torque from the estimated biceps torque (Eq 4). **E)** Angular velocity resulting from the admittance model (Eq 5). **F)** Elbow angle displacement resulting from the integral of the angular velocity (Eq 5).